

Electrical and mechanical study of a medium-voltage overhead distribution line

Cossi Télésphore Nounangnonhou^{1,2}, Guy Clarence Semassou¹, Kossoun Alain Tossa¹, and Maryse Assogba¹

¹Laboratory of Energetics and Applied Mechanics (LEMA), University of Abomey-Calavi, Benin

²Laboratory of Electrotechnics, Telecommunications and Applied Informatics (LETIA), University of Abomey-Calavi, Benin

Copyright © 2024 ISSR Journals. This is an open access article distributed under the *Creative Commons Attribution License*, which permits unrestricted use, distribution, and reproduction in any medium, provided the original work is properly cited.

ABSTRACT: The Benin Sustainable and Secure Access to Electrical Energy Project (PADSBEE), initiated by the Government of Benin, aims to develop sustainable access to electricity through the construction of new lines to extend distribution networks. The construction of overhead distribution lines requires perfect knowledge and application of the climatic, electrical and geometric constraints to which they are subject. Our work thus consists in designing a software package for the electrical and mechanical dimensioning of medium-voltage overhead lines, with its application to the 3 km long 20 kV overhead line in the town of Come, in the Mono department. Based on the characteristics of the conductor to be used, the current criteria and the maximum permissible voltage drop, the electrical dimensioning allowed us to determine an Almelec conductor with a cross-section of 75.5 mm² and composite insulators with a 490 mm creepage distance. From a mechanical point of view, verification of clearances to obstacles led to the selection of reinforced concrete supports 12 m in line and at a standstill, and 13 m at an angle. Wind and conductor loads on the supports led to the selection of Class A supports with a force of 300 daN in alignment, a Class A support with a force of 800 daN at an angle, and Class C supports with a force of 2000 daN at a stop. Reinforcements are of the sheet-vault type in alignment, horizontal stirrup in angle and single cross-member anchorage in stop.

KEYWORDS: Medium voltage; power line; dimensioning; software; reinforced concrete.

1 INTRODUCTION

The provision of energy services is essential for the social and economic well-being of populations. In developing countries, the situation of access to electricity remains highly contrasted between urban and rural areas. With a national electricity access rate of 30.39%, 5.70% in rural areas and 57.36% in urban areas, Benin shows in 2020 a growing imbalance between the rapid development of urban areas and the socio-economic situation of rural areas¹. Mindful of this situation, the Beninese government has decided to sand up the Benin Sustainable and Secure Access to Electrical Energy Project (PADSBEE). The main objective of this project is to develop sustainable access to quality electricity for domestic, commercial and industrial use, in compliance with safety, environmental and social standards. Through the implementation of this project, Benin aims to achieve a national coverage rate of 75% by 2025, including 50% in rural areas and 90% in urban areas, and to ensure that the voltage plan is maintained at all nodes². The distribution component of this project involves the construction of new lines for the Reinforcement, Densification and Upgrading (RDMN) of the distribution network for which Beninese Electric Power Company (SBEE) is the concessionaire. Generally speaking, the construction of overhead lines for medium-voltage distribution networks varies according to the location, energy requirements and construction assumptions. Consideration of the elements involved and the severity of the electrical, geometrical and climatic constraints to which overhead lines are subjected are important factors in the choice of the various components that make them up³. For this reason, it is essential to carry out a good electrical and mechanical study of medium-sized overhead distribution lines in order to guarantee quality service at an affordable price.

A great deal of work has already been done on the electrical and mechanical design of overhead medium-voltage distribution lines⁴. Notably in the sub-region, such as in Burkina-Faso for the construction of the 33 kV inter-urban PA-DEDOUGOU power link, for the construction of the 15 kV Bobo-Dioulasso power distribution line⁵, for studies to supply MV/LV substations in the city of OUAGADOUGOU or for the construction of a 20 kV line in the Maourey housing estate^{4,5,6,7}. In Togo, with the design of a software package for electrical and mechanical calculations of overhead distribution lines; and even in Benin, with the construction of 33 kV HTA power lines in the north^{8,9}. However, the mechanical calculation method for supports and fittings does not correspond to that developed by standard NFC

11-201 (which defines the construction rules for overhead power lines in medium-voltage distribution networks¹⁰. The NFC 11-201 standard takes account of stresses along the axes of the line elements. What's more, these various projects were carried out under different constraints (electrical, climatic and geometric). For this reason, the technical specifications for the PADBSEE project recommend the use of the NFC 11-201 standard.

The present work involves an electrical and mechanical study of overhead medium-voltage distribution lines.

Table 1. Nomenclature

Elements	Symbols	Units (SI)
Staking angle	β	°
Coefficient of linear expansion	α	-
Coefficient of simultaneity	k_s	-
Coefficient of transverse support force	τ	-
Downgrading coefficient	η	-
Temperature coefficient	ζ	K ⁻¹
Short-circuit current	I_{cc}	A
Permissible current	I_{ad}	A
Rated current	I_n	A
Horizontal transverse force	h	N
Horizontal longitudinal	i	N
Vertical force	Q	N
Wind load along the axis of the large support inertia	Z_H	N
Wind force along axis of small support inertia	Z_I	N
Deflection	F	M
Height	H	M
Vanishing line	L_f	cm

2 MATERIALS AND METHODS

2.1 MATERIALS

In order to carry out this study we used:

- VBA Excel;
- MATLAB.

2.2 METHODS

2.2.1 METHOD USED FOR THE ELECTRICAL DIMENSIONING OF A MEDIUM-VOLTAGE OVERHEAD LINE

The electrical sizing of a medium-voltage overhead line involves determining the conductor characteristics (material, cross-section) and the insulator characteristics.

2.2.1.1 SIZING THE ELECTRICAL CONDUCTOR

2.2.1.1.1 CHOICE OF MATERIAL

The choice of material for the electrical study of conductors is essential. Line losses depend on the type of conductor. For the same transmission distance, line losses and voltage drop are greater when the resistivity of the conductor used is higher. On the other hand, influencing the cross-section of these conductors can help reduce resistance; however, this is not economical, as the larger the conductor cross-section used, the greater the weight of the conductor and the greater the need for oversized insulators and supports, which exaggerates the cost of line construction. Conductors must therefore be carefully selected to optimize construction costs, operating costs and line losses¹¹.

Electrical conductors must:

- Have good electrical conductivity;
- Have good tensile strength;
- Be economical;
- Have good surface hardness;
- Be lightweight;
- Good corrosion resistance.

Table 1 below shows the advantages and disadvantages of the most commonly used materials.

Table 2. Advantages and disadvantages of materials⁶

Materials	Advantages	Disadvantages
Steel	<ul style="list-style-type: none"> - Withstands attraction (Good mechanical strength) - Good price 	Very poor resistivity
Copper	<ul style="list-style-type: none"> - Good resistivity - Good mechanical strength 	High price
Aluminum	<ul style="list-style-type: none"> - Good resistivity - Acceptable price 	<ul style="list-style-type: none"> - Does not withstand attraction (poor mechanical strength) - Low breaking load - Used for small doors

From analysis of table 1 above, we can deduce that copper is an ideal material because of its good resistivity and mechanical strength. In addition, it has a high current density, with a fairly high current-carrying capacity of copper per unit cross-section¹². However, due to its high cost and unavailability, it is rarely used. For these reasons, the use of aluminum is prioritized. Aluminum has an economic advantage in terms of price and ease of processing. To increase its hardness and mechanical strength, aluminum is treated and combined with other materials. The result is hard-drawn aluminum, annealed aluminum and alloyed aluminum (almelec).

Table 2 below shows the characteristics of the various materials used to select the conductor to be used.

Table 3. Characteristics of different materials³

Materials	Hard drawn aluminum	Almélec	Annealed aluminum
Resistivity at 20°C (10 ⁻⁸ Ωm)	2.825	3.26	2.92
Stress at break (MPa)	160 to 180	315 to 325	59 to 97
Elongation at break	1 %	3 %	~ 20 %
Maximum temperature (°C)	75	75	250

2.2.1.1.2 DETERMINING CONDUCTOR CROSS-SECTION

To determine the conductor cross-section, we evaluated the power absorbed on the network using the power balance in order to determine the conductor cross-section according to three criteria:

- Rated operating current I_n ;
- I_{cc} short-circuit current criterion;
- Voltage drop criterion

1) Determination of the power absorbed on the network P_m

$$P_m = P_u(1 + \alpha)^n \tag{1}$$

2) Rated current criterion

$$I_n = \frac{P_m}{\sqrt{3} \cdot U_n \cdot \cos \phi} \tag{2}$$

$$I_{ad} = K \cdot S^{0,62} \tag{3}$$

$$\text{with } I_n \leq I_{ad} \tag{4}$$

3) Short-circuit current criterion

$$I_{cc} = \frac{U_n}{Z_{eq} \cdot \sqrt{3}} \tag{5}$$

$$I \frac{S \cdot a}{\sqrt{t_{cc} c_{cmax}}} \tag{6}$$

$$I_{cc} \leq I_{ccmax} \tag{7}$$

4) Voltage drop criterion

$$\frac{\Delta U}{U} = \frac{\sqrt{3} \cdot I (R \cos \phi + X \sin \phi)}{U} \tag{8}$$

with: $\frac{\Delta U}{U} \leq 5\%$ (9)

- P_u : power used on the grid [kW];
- U_n : nominal line voltage [kV];
- S : conductor cross-section [mm²];
- K : coefficient depending on the nature of the conductor material;
- $\cos \phi$: power factor;
- Z_{eq} : equivalent impedance of all impedances through which the short-circuit current flows [Ω];
- U_n : nominal mains voltage;
- S : cable cross-section [mm²];
- t_{cc} : short-circuit time, often taken to be 1s;
- a : factor depending on the nature of the conductor¹²;
- $a = 105.3$ for copper
- $a = 55.07$ for aluminum
- $a = 61.98$ for almelec

Table 4. *K factor*¹³

K	Copper	Almelec	Alu-Steel
	21	17.1	16.4

2.2.1.2 INSULATOR SIZING

Insulator sizing depends on the type of material, the installation area, the leakage length and/or the number of plates.

2.2.1.2.1 CHOICE OF MATERIAL

The insulator must:

- Have good mechanical strength;
- Have good insulation resistance;
- Be economical;
- Be lightweight;
- have good corrosion resistance

The choice of material was based on an analysis of the advantages and disadvantages of the three (03) materials used to manufacture insulators, as shown in Table 4 below.

Table 5. Advantages and disadvantages of each isolator¹³

Materials	Advantages	Disadvantages
Ceramic	Can withstand high mechanical stress	High cost
Glass	- Low cost - Easy to observe defects - Can withstand sudden temperature changes	- Heavy and difficult to handle - Can only withstand low mechanical stress
Composite	- Lightweight - High mechanical strength suitable for heavily polluted areas - Medium cost	- Invisible aging

2.2.1.2.2 DETERMINING THE MINIMUM CREEPAGE DISTANCE

The creepage distance of an insulator is the most important parameter determining its electrical performance. It represents the distance measured across the surface of the insulating material. The creepage distance depends on the weather conditions on site.

The minimum creepage distance L_f is determined by the following formula:

$$L_f = 1.1 \times U_M \times \varphi \tag{10}$$

With:

- U_M : Highest voltage allowed by the equipment [kV];
- φ : bypass voltage [cm/kV]

2.2.2 METHOD USED FOR THE MECHANICAL DIMENSIONING OF A MEDIUM-VOLTAGE OVERHEAD LINE

The mechanical design of overhead medium-voltage distribution lines involves determining the mechanical characteristics of conductors, the size of supports and the choice of fittings.

2.2.2.1 DETERMINING CONDUCTOR CHARACTERISTICS

The mechanical calculation of conductors involves studying variations in mechanical stress and determining conductor deflections.

2.2.2.1.1 DETERMINING THE CONDUCTOR'S FINAL MECHANICAL STRESS

We determined the conductor's final mechanical stress t_f from the change-of-state equation presented by the following expression:

$$t_f^3 + t_f^2 \left[\frac{E \times a_{\acute{e}q}^2 \times m_i^2 \times w^2}{24 \times t_i^2} + E \times \alpha (\theta_f - \theta_i) - t_i \right] = \frac{E \times m_f^2 \times a_{\acute{e}q}^2 \times w^2}{24} \tag{11}$$

With:

- θ : temperature;
- t : mechanical tension;
- $a_{\acute{e}q}$: equivalent span;
- m : overload coefficient;
- α : coefficient of linear expansion;
- w : specific weight of conductor;
- E : modulus of elasticity;

The final mechanical stress of the conductor is that of the most restrictive climatic assumption not exceeding $\frac{1}{k_1}$ of the conductor breaking load⁴. This tension is used to determine the support gauge.

2.2.2.2 DETERMINING THE SUPPORT TEMPLATE

2.2.2.2.1 CHOICE OF SUBSTRATE TYPE

Supports must have the following properties:

- High mechanical strength to support conductor and wind loads;
- Low purchase and maintenance costs;
- Long service life;
- Easy maintenance of conductors.

The choice of supports was made between wood, concrete and mandal.

Table 6. Characteristics of substrate types¹⁴

Nature	Advantages	Disadvantages
Wood	<ul style="list-style-type: none"> • Substantially lower overall line cost than concrete or steel supports; • Lighter than concrete or mandal equivalents; • Easier to handle than other supports; • Easy to climb 	<ul style="list-style-type: none"> • Susceptible to termite attack; • Susceptible to severe splitting, depending on wood type and origin; • Normally require guying or bracing at corners and stops; • Likely to catch fire in the event of fire or insulation failure;
Concrete	<ul style="list-style-type: none"> • Aesthetics ; • Long service life ; • Maintenance-free once installed; • They are self-supporting (no shoring or bracing required); • Better local content (cement, iron, labor, etc.); • Very high mechanical strength. 	<ul style="list-style-type: none"> • Largely disadvantaged compared to wood or steel structures in terms of transport, handling and erection, due to their high mass and fragility; • Problems associated with their manufacture (absence of material resistance tests during construction; careless selection and mixing of materials; insufficient drying period, etc.);
Mandal	<ul style="list-style-type: none"> • Long service life • Use of long spans ; • Easy to transport and erect; • Low maintenance; • Self-supporting. 	<ul style="list-style-type: none"> • No local content; • Requires reinforced concrete foundations; • More expensive than other types of support; • Subject to corrosion;

2.2.2.2.2 DETERMINING THE RESULTING SUPPORT FORCE

The resulting stress on the support represents the forces applied to the power line support, i.e.:

- The forces due to the conductors;
- Wind load on the support and on the fittings (armatures and insulators)

The resultant R on the support is determined by the formula below:

$$R = F_f + \frac{|H| + Z_H + \frac{|I| + Z_I}{\tau}}{\eta} \tag{12}$$

Where:

$$I = n \cdot \left(\left[V \left(\frac{a_j}{2} - \frac{a_i}{2} \cdot \cos \beta \right) \right] \sin \frac{\beta}{2} + [(T_i - T_j)] \cos \frac{\beta}{2} \right) \tag{13}$$

$$H = n \cdot \left(\left[V \cdot \left(\frac{a_i}{2} \cdot \cos^2 \beta + \frac{a_j}{2} \right) \right] \cdot \cos \frac{\beta}{2} + [(T_i + T_j)] \sin \frac{\beta}{2} \right) \tag{14}$$

$$Z_H = r \cdot V_V \cdot \cos^2 w' \tag{15}$$

$$Z_I = r \cdot V_V \cdot \sin^2 w' \tag{16}$$

With:

- F_f : flat-rate force (for fittings, the following flat-rate values are used: $F_{ferrures} = 15 \text{ daN at } 180 \text{ Pa, } 25 \text{ daN at } 480 \text{ Pa, } 30 \text{ daN at } 585 \text{ Pa}$ and $35 \text{ daN at } 640 \text{ Pa}$);
- H and I : conductor forces on the support's axes of inertia;
- Z_H and Z_I : wind components on the support;
- τ : coefficient of the transverse force of the support;
- η : derating coefficient taking into account the offset of the bearing point of the forces due to the conductors in relation to the standardized reference, which is 0.25m below the top of the support;
- a_i : smallest span; a_j : largest span;
- V : wind load on conductor;
- β : staking angle;
- V_V : conventional wind force;
- r : wind pressure correction coefficient according to the hypothesis considered ($= \frac{P_h}{P}$);
- P_h : wind pressure in the hypothesis considered;
- P : Wind pressure for assumption A in normal wind zone;
- w' : angle of the wind direction on the support with its axis of great inertia

$$w' = \frac{\pi}{2} - \Omega + \frac{\beta}{2} \tag{17}$$

- Ω : orientation angle: angle made by the support's axis of great inertia with the bisector of the staking angle (0° in stop; 90° in alignment; β in angle¹⁵)

We look for the support with the force immediately greater than the calculated force.

2.2.2.2.3 MINIMUM CONDUCTOR ATTACHMENT HEIGHT

The minimum conductor attachment height H depends on the ground clearance G , the conductor deflection f and the installation height h_0 . It is determined by the following formula:

$$H = G + f_m + h_0 \tag{18}$$

- With: G : ground clearance;
- f_m : maximum deflection;
- h_0 : installation height.

This value is used to select the total height of the support.

2.2.2.3 DETERMINING THE ARMING GAUGE

The choice of armament depends on the function of the support, the span of the line or the distance between conductors. The following Table 6 shows the criteria for selecting the armatures generally used.

Table 7. Armament selection¹³

Support function	Span	Armament type
Alignment	$\leq 60 \text{ m}$	- Flag - Alternating
	$> 60 \text{ m}$	- Vaulted-tablecloth
Angle	$\leq 10 \text{ Gr } (9^\circ)$	- Flag - Tablecloth
	$>10 \text{ Gr } (9^\circ)$	- Harrow (crosspiece for TAD dual anchorage) - Suspension bracket ETA (CUO)
Stop	-	- Herse (crossbar for single anchorage TAS) - Suspension bracket ETA (CUO)

The loads applied to an armature at each of a conductor's attachment points are determined by the following formulas:

- h: Horizontal force

$$h = V \left(\frac{a_i}{2} \cdot \cos^2 \beta + \frac{a_j}{2} \right) \cdot \cos \frac{\beta}{2} + (T_i + T_j) \sin \frac{\beta}{2} \quad (19)$$

- q: Vertical force

$$q = p \left(\frac{a_i}{2} + \frac{a_j}{2} \right) + T_i - T_j \quad (20)$$

With:

- p : linear weight of conductor

To facilitate the electrical and mechanical study, we have designed a software package using the VBA language. Figure 1 below shows the software's main menu.

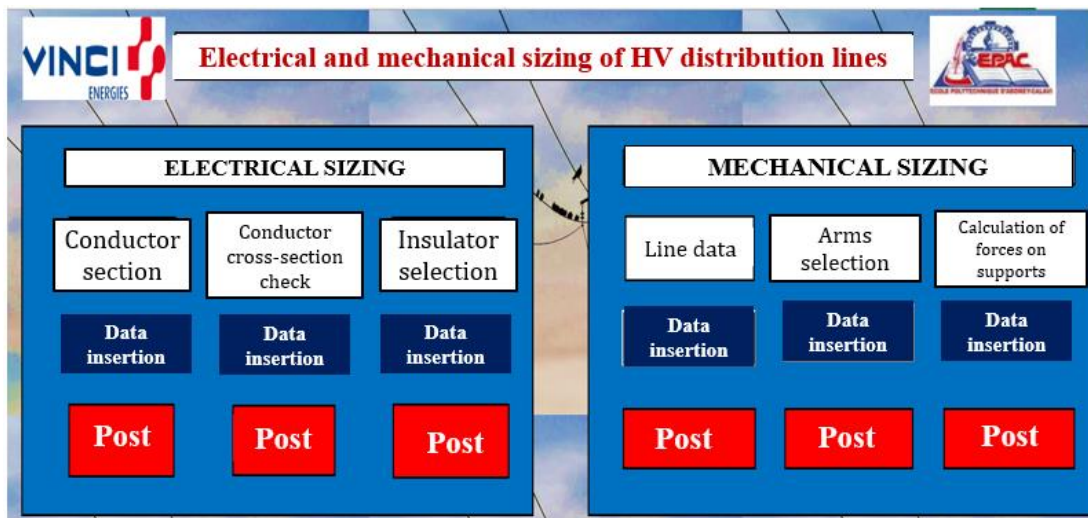


Fig. 1. Software main menu

Figures 2 and 3 below show the software's electrical and mechanical operating diagrams.

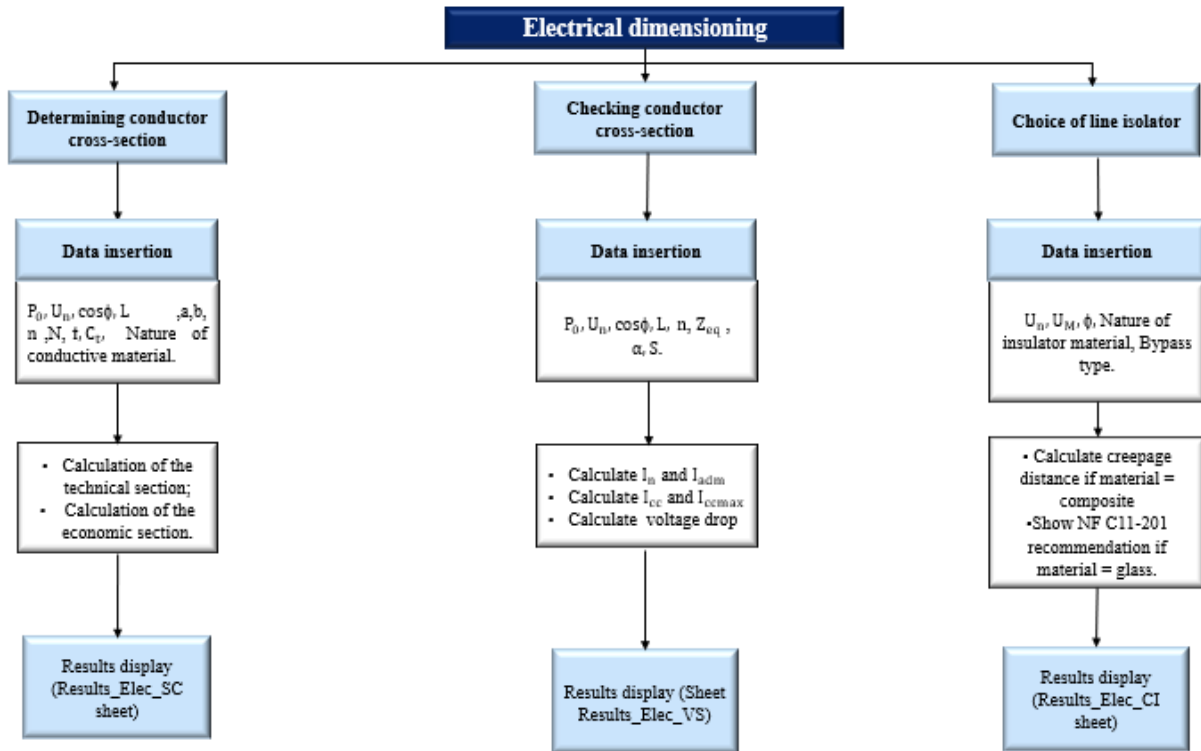


Fig. 2. Electrical sizing flow chart

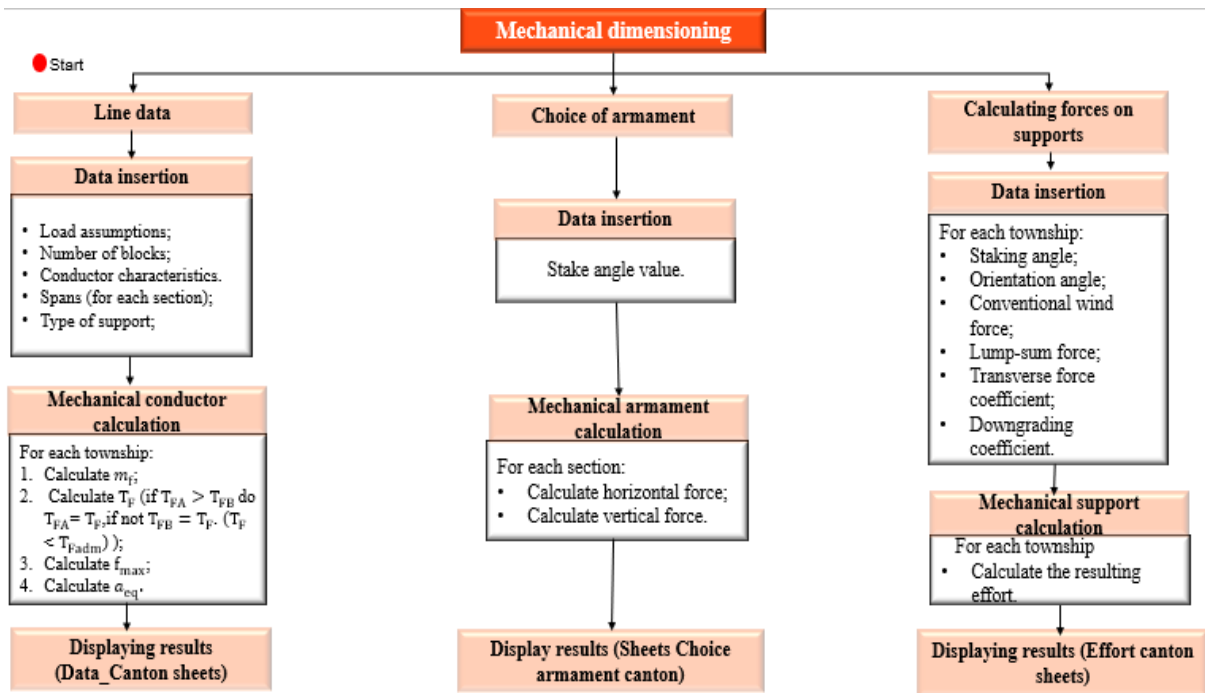


Fig. 3. Mechanical sizing flow chart

2.2.2.4 OPTIMIZING A CLASS A CORNER SUPPORT

The size of the support is a decisive factor in the economic evaluation of overhead power line construction. Indeed, the greater the resultant force on the support, the greater the support gauge. However, when we speak of gauge, we are referring to the quantities of materials (cement, sand, gravel, etc.) used in the production of the support; this creates a relationship between gauge and quantity of mass (production cost).

Figure 4 below shows the variation in the quantity of aggregate used as a function of support effort.

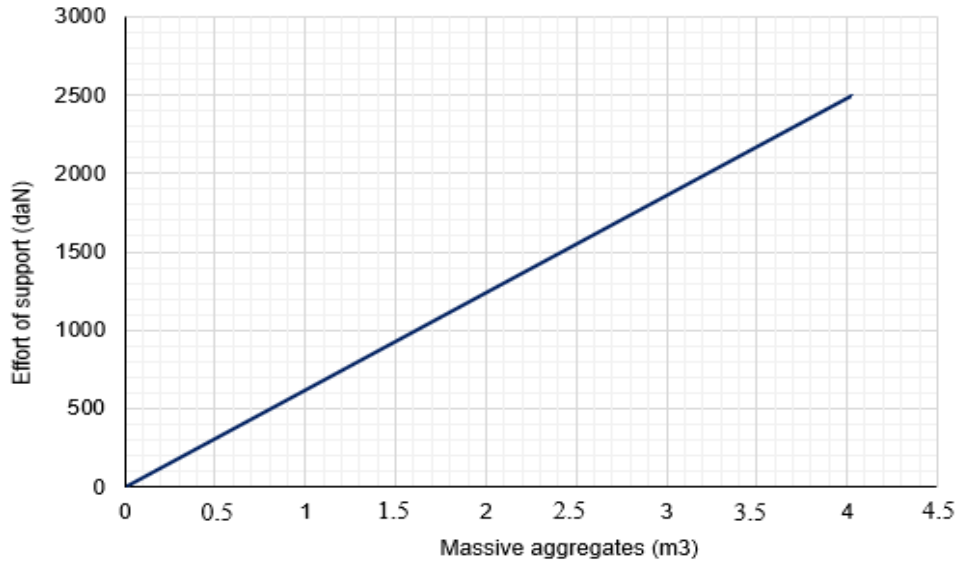


Fig. 4. Massive aggregates as a function of support force¹⁶

It can be seen from this figure that the greater the support effort, the greater the quantity of massifs; it is therefore important to make a judicious choice of support gauge to optimize the cost of overhead line construction.

We have studied the influence of span a and staking angle β on the value of the resultant R (see equation 8) of the forces of a corner support ($R = f(a, \beta)$).

For the resolution of the resultant R , we have taken into account the following values and variables:

- Values

$$F_f = 35 \text{ daN}; \eta = 1; \tau = 0.30.$$

- Variables

$$H = 3 \cdot \left[0.36 \cdot (a \cdot \cos^2 \beta + a) \cdot \cos \frac{\beta}{2} + 2T \cdot \sin \frac{\beta}{2} \right] \quad (21)$$

$$I = 3 \cdot \left[0.36 \cdot (a - a \cdot \cos^2 \beta) \cdot \sin \frac{\beta}{2} \right] \quad (22)$$

$$Z_H = 66.5 \cdot \cos^2 \left(\frac{\pi - \beta}{2} \right) \quad (23)$$

$$Z_I = 66.5 \cdot \sin^2 \left(\frac{\pi - \beta}{2} \right) \quad (24)$$

Solving this equation led to the development of a MATLAB code. The various developments carried out within the MATLAB code enable us to determine the values of the stress on the support.

3 RESULTS AND ANALYSIS

Copper is an ideal material because of its good resistivity and mechanical strength. In addition, it has a high current density, with a fairly high current-carrying capacity of copper per unit cross-section¹². However, due to its high cost and unavailability, it is rarely used. For these reasons, the use of aluminum is prioritized. Aluminium has an economic advantage in terms of price and ease of processing. To increase its hardness and mechanical strength, aluminum is treated and combined with other materials, as shown in Table 1. Analysis of this table allows us to choose an Almelec phase conductor. Almelec has a higher mechanical strength ($3.26 \cdot 10^8 \Omega \text{m}$ à 20°C) than hard-drawn aluminum ($2.825 \cdot 10^8 \Omega \text{m}$ à 20°C) and annealed aluminum ($2.92 \cdot 10^8 \Omega \text{m}$ à 20°C). Its surface hardness is higher, roughly twice that of aluminum wire, which makes it less susceptible to injury during unwinding, thus reducing corona losses. What's more, its

homogeneous nature makes it perfectly resistant to corrosion, and stresses are more evenly distributed in the cross-section, not to mention its weight, which offers the best compromise of all.

Once the nature of the conductor had been chosen, based on the power absorbed on the network, we checked whether the 75.5 mm² cross-section met the needs of the town of Com e.

To serve 1,000 households, the network requires a power of **4843.80 kW**, i.e. a rated current of **155.36 A**, over a 20-year service life. A 75.5 mm² conductor, on the other hand, can only accept a maximum current of **249.65 A**. It can be seen that the admissible current of the 75.5 mm² conductor is much higher than the nominal network current ($I_{ad}(249.65 A) > I_n(155.36 A)$). This means that the rated current criterion has been met.

Comparing the admissible short-circuit currents of the network and the conductor (**2886.75 A** and **4679.49 A** respectively), we see that the short-circuit current criterion ($I_{ccmax}(4679.49 A) > I_{cc}(2886.75 A)$) is met.

Finally, the voltage drop generated by the cable along the **4.6%** line does not exceed that predicted by Benin **5%**: the voltage drop criterion has been met.

The simultaneous verification of the three criteria allows us to approve the conductor cross-section of 75.5 mm²; we therefore maintain this cross-section as the line's phase conductor.

The choice of a composite insulator is justified by its ability to establish a flexible connection between conductors and their supports, thus enabling better distribution of forces between spans, and by its high mechanical strength and medium cost compared with other types. Based on the line operating voltage equivalent to 24 kV and the average pollution level in the area corresponding to a creepage distance of 20 mm/kV, we obtained a creepage distance of **483.12 mm** for the insulator.

The line will be protected by an IACM 24kV/50A manually operated overhead switch installed at the start of the line. The downstream cables will be protected by a set of 3 surge arresters and 3 fuses; the arresters will be of the zinc oxide type with synthetic envelope.

The type of support chosen for the line is reinforced concrete. The choice because of its high mechanical strength, aesthetic appeal and long service life. Compared with other types of support, it requires no maintenance. What's more, the disadvantages of this type of support are manageable, not to mention the fact that it has better local content. Verification of the regulatory distances to the maximum deflection resulted in a total height of 12m for the aligned and stopped supports, and 13m for the angled support.

The reinforcement calculations led to the selection of NV1 50-50 sheet-arch reinforcement for the aligned supports, ETA hooking stirrup reinforcement for the angled support and single-anchored transverse harrow reinforcement (TAS) for the stopped supports.

Calculation of the forces on the supports yielded values ranging from 279.29 daN to 286.49 daN for the aligned supports. We therefore take the normalized force immediately above the values found, i.e. 400 daN. The same exercise was carried out for brackets at a standstill. However, the values obtained, 5407.57 daN and 5417.13 daN, are not part of the normalized force values for Class A reinforced concrete supports. We therefore substituted Class C supports of 2000 daN. For the corner support, we have chosen a Class A support with a force of 800 daN. The support manufacturer must take into account the breaking load of the supports with breaking load \geq support load * 2,1 .

Figures 5 and 6 show the force variation curves for a Class A angle support as a function of span and staking angle respectively. Table 6 shows the variation in force as a function of angle and span.

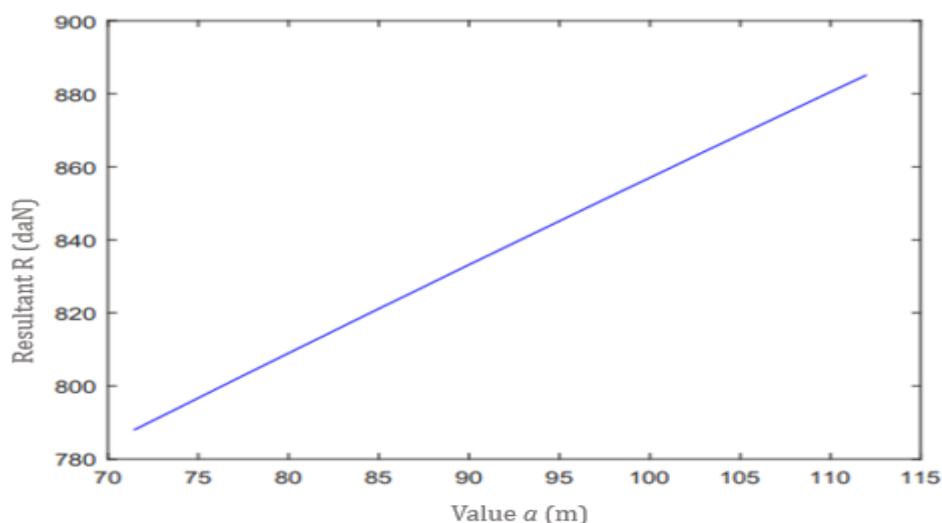


Fig. 5. Variation of Class A corner support force as a function of span

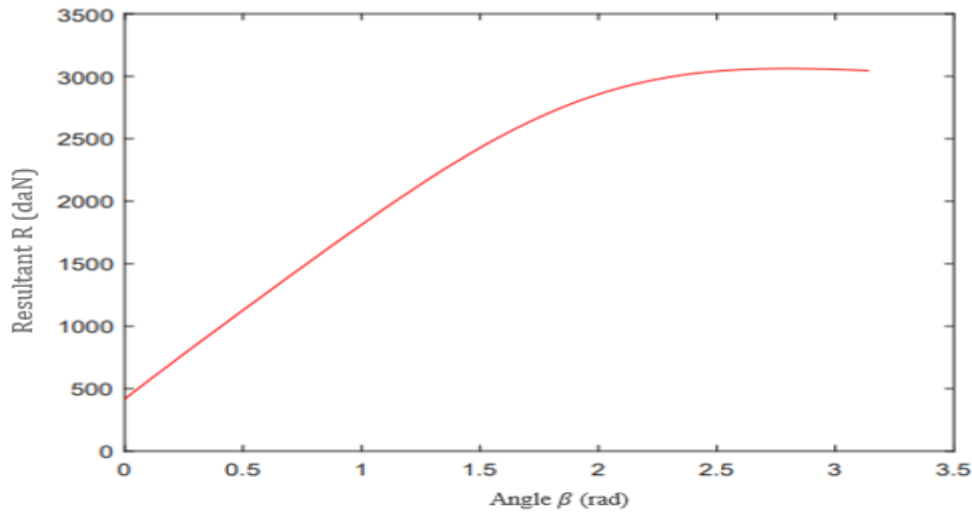


Fig. 6. Variation of Class A corner support force as a function of staking angle β .

Figure 5 shows the variation of the resultant force of the corner support as a function of span. From this graph, it can be seen that the greater the span, the greater the value of the resultant R. Figure 6 shows the variation in the resultant force of the corner support as a function of the staking angle. It can be seen from this graph that the greater the staking angle, the greater the value of the R resultant. We can therefore deduce that the staking angle and the line span have a major impact on the choice of angle support force. In order to determine which parameter has the greatest impact, we evaluate the variation of the support force as a function of angle and span, as shown in Table 7 below. Figure 6 shows the variation in the resultant force of the corner support as a function of the staking angle. It can be seen from this graph that the greater the staking angle, the greater the value of the R resultant. We can therefore deduce that the staking angle and the line span have a major impact on the choice of angle support force. To determine which parameter has the greatest impact, we evaluate the variation in support force as a function of angle and span, as shown in Table 7 below.

Table 8. Table 7: Variation of force as a function of angle and span.

Span a (m)	70	111
Staking angle β		
0°	151.2 daN	239.76 daN
	1970.79 daN	1987.94 daN
90°	2121.99 daN	2227.70 daN
		148.71 daN

Analysis of Table 7 shows that the differences in force values for fixed angles and varied spans (88.56 daN and 148.71 daN) are smaller than the differences in force values for fixed spans and varied angles (1970.79 daN and 2227.70 daN); we therefore conclude that the staking angle is the most sensitive parameter in the choice and calculation of the force of a corner support.

For technico-economic optimization, we propose that in the choice of the optimum line layout, the use of angle values $\beta < 90.8^\circ$ for Class A corner supports should be taken into account.

For a Class A corner support with:

- a staking angle $\beta > 16^\circ$, a force $F=800$ daN is sufficient;
- a staking angle $16^\circ \leq \beta < 19.3^\circ$, a force $F=1000$ daN is sufficient;
- a staking angle $19.3^\circ \leq \beta < 33.9^\circ$, an effort $F=1250$ daN is sufficient;
- a staking angle $33.9^\circ \leq \beta < 46.5^\circ$, $F=1600$ daN is sufficient;
- a staking angle $46.5^\circ \leq \beta < 71.62^\circ$, an effort $F=2000$ daN is sufficient;
- a staking angle $71.62^\circ \leq \beta < 90.8^\circ$, an effort $F=2500$ daN is sufficient

4 CONCLUSION

The electrical study of the line consisted in selecting the phase conductor and insulators. This study revealed the use of bare 75.5 mm² Almelec conductors and composite insulators with a 490 mm creepage distance for a mechanical load of 70 kN. As for the mechanical study, it enabled us to determine the various forces exerted on the conductors, the armatures and the supports in order to define the gauge of the supports and armatures to be used. Reinforced concrete supports were chosen for this project. These supports are grouped into three categories, according to the forces applied to them and their function on the line. These are: alignment supports 12 A 400 daN (height 12 m, class A, force 400 daN) with NV1 50-50 sheet-arch reinforcement, a corner support 13 A 800 daN with CUO horizontal clamp reinforcement and stop supports 12 C 2000 daN with single-anchor harrow reinforcement. Also, in the distribution of supports for overhead medium-voltage distribution lines, it is preferable to avoid angles; for a Class A corner support, angle values $\beta < 90.8^\circ$ are recommended.

REFERENCES

- [1] Ministère de l'Énergie du Bénin. Politique nationale de maîtrise d'énergie 2020-2030. https://pspdb.dev.gouv.bj/server/storage/app/PolitiqueFichiers/63_PONAME_VF.pdf. 26 mai 2023.
- [2] Ministère de l'Énergie du Bénin. Projet d'Accès Durable et Sécurité du Bénin à l'Énergie Électrique (PADSBEE 2019-2025). <https://energie.gouv.bj/page/projet-dacces-durable-et-securise-du-benin-a-lenergie-electrique-padsbee-2019-2025>. 15 juillet 2022.
- [3] Médiapart Bénin. Mise en œuvre du PADSBEE : Objectif, 75% de taux d'accès à l'électricité d'ici 2025. <https://mediapartbenin.com/article/675/benin-mise-en-%C5%93uvre-padsbee-objectif-75%25-taux-acces-a-electricite-ici-2025/>. 31 mars 2022.
- [4] Zougba I. (2013). Etude et dimensionnement de la liaison électrique interurbaine Pa-Dédougou : Tronçon 33kV Safané-Wona. Mémoire de Master en génie électrique, énergétique et énergie renouvelable. Institut International d'Ingénierie de l'Eau et de l'Environnement (2IE), Ouagadougou, Burkina Faso.
- [5] Ye J. R. (2019). Construction d'une ligne de distribution électrique hta de 15 kV et restructuration d'un réseau électrique bta au secteur 30 de bobo-dioulasso (Mémoire d'Ingénieur avec grade de Master en génie électrique et énergétique). Institut International d'Ingénierie de l'Eau et de l'Environnement (2IE), Ouagadougou, Burkina Faso.
- [6] Madeca M. M. (2019). Etudes techniques d'alimentation de postes hta/bta sur portique dans la ville de ouagadougou : cas du poste 122 à nonsin (Mémoire d'Ingénieur avec grade de Master en génie électrique et énergétique). Institut International d'Ingénierie de l'Eau et de l'Environnement (2IE), Ouagadougou, Burkina Faso.
- [7] Houssamatou Doudou M. K. (2018). Étude de la construction d'une ligne haute tension catégorie A (20 kV) et la conception d'un réseau HTA/BT pour l'alimentation en énergie électrique de la cité MAOUREY. (Mémoire d'ingénieur avec grade Master en génie électrique et énergétique). Institut International d'Ingénierie de l'Eau et de l'Environnement (2IE), Ouagadougou, Burkina-Faso.
- [8] Alvarez-Hérault M.-C. (2009). Architectures des réseaux de distribution du futur en présence de production décentralisée (Thèse de doctorat en génie électrique). Institut polytechnique de Grenoble, Grenoble, France.
- [9] Moustapha A. (2011). Projet d'alimentation électrique de la localité de Yaba: Construction d'une ligne d'interconnexion HTA 33kV and le réseau HTA/BTA de Yaba (Mémoire de Master en génie énergétique et énergie renouvelable). Institut International d'Ingénierie de l'Eau et de l'Environnement (2IE), Ouagadougou, Burkina-Faso.
- [10] Tefegium V. S. (2014). Etude de la construction d'une ligne électrique haute tension 90 kV PA-WONA (Mémoire de Master en Génie électrique et énergétique). Institut International d'Ingénierie de l'Eau et de l'Environnement (2IE), Ouagadougou, Burkina Faso.
- [11] TUO K. (2020). Etude électrique et mécanique d'une ligne électrique aérienne interurbaine HTB 90 kV KOSSODO-ZINIARE (Mémoire d'ingénieur avec grade Master en génie électrique et énergétique). Institut International d'Ingénierie de l'Eau et de l'Environnement (2IE), Ouagadougou, Burkina Faso.
- [12] Belaid F. (2014). Contribution au dimensionnement des lignes électriques de transport de l'électricité (Mémoire de Fin d'Etudes de Master professionnel en Génie Electrique). Université Mouloud Mammeri de Tizi-Ouzou, Algérie.
- [13] Avril C. (1974). Construction des lignes aériennes à haute tension, Edition Eyrolles, 61, boulevard Saint-Germain, Paris V^e p. 623.
- [14] N'diaye Modou (2000). Problématique de la conception d'un nouveau type de poteau pour les réseaux d'électrification rurale au Sénégal (Mémoire d'ingénieur de conception en électromécanique). Ecole Polytechnique de Thiès, Université Cheikh Anta Diop, Sénégal.
- [15] Enedis. Manuel utilisateur Camelia (version 4,5). https://www.alpamayo.fr/images/uploads/camelia/Camelia-Calcul_v4.50_Manuel-Utilisateur.pdf. 13 juin 2022.
- [16] Hatim A. et Salim R. (2015). Etude de la téléconduite des OCR et de la DPS (Rapport de stage de fin d'étude en Licence des Sciences et Techniques, option: électronique, électrotechnique et automatique). Université Hassan 1^{er}, Maroc.